Polymer Chemistry

ROYAL SOCIETY OF CHEMISTRY

PAPER

View Article Online
View Journal

Cite this: DOI: 10.1039/d6py00258g

Investigating the synthesis, properties and Diels–Alder reactivity of diene-functional branched polyesters using copolymerisation of furfuryl methacrylate under transfer-dominated branching radical telomerisation (TBRT) conditions

Oliver B. Penrhyn-Lowe,[a] Stephen Wright,[a] Sarah Lomas,[c] Andrew T. Slark,[b] Andrew B. Dwyer[a] and Steve P. Rannard *[a]

Received 16th March 2026,
Accepted 7th May 2026

DOI: 10.1039/d6py00258g

rsc.li/polymers

Diels–Alder reactions have been of considerable interest for many years and strategies for polymeric diene synthesis have predominantly relied on controlled radical polymerisation techniques to avoid unwanted side reactions of furan rings. Alternatively, modification of step-growth polymers or syntheses has been employed to introduce furans into step-group backbones or as pendant groups. Here we have used conventional free radical chemistries employed under TBRT conditions to synthesise branched furan-functional polyester resins with pendant furan rings using furfuryl methacrylate as a feedstock. No adverse side reactions were evident and the resulting high molecular weight polymers were readily able to undergo reversible gelation, using a commercially available bismaleimide, thereby opening new avenues for Diels–Alder resin design.

Introduction

Reversible chemistries, those exhibiting a dynamic equilibrium, have interested chemists for over 200 years with Berthollet first recognising reversible salt reactions and Le Chatelier later formalising these principles. In the late 1920s, seminal work by Otto Diels and Kurt Alder introduced the [4 + 2] diene/dienophile cycloaddition reaction to the chemistry community, receiving their joint Nobel Prize in 1950.[1] Interestingly, the researchers also attempted to prevent others from utilising this now ubiquitous reaction, stating in their 1928 paper, "*We expressly reserve the right to apply the reactions we have discovered*...".[2]

Diels–Alder (D–A) chemistry has found utility in a wide range of research fields including the total synthesis of natural compounds,[3] drug delivery applications,[4] agrochemistry,[5] profragrance chemistry,[6] and nanomaterials.[7] Within polymeric materials science, D–A reactions have seen application in backbone formation, coupling to form block, graft and cyclic copolymers, dendrimer synthesis, self-healing polymers, gels, and coatings.[8–12] In his 75th anniversary review of D–A chemistry, Corey stated it is "*one of the most important and fascinating transformations in chemistry,...[that]...continues to surprise, excite, delight, and inform the chemical community*".[13]

Furan-derived dienes feature commonly in D–A reactions and may be introduced into macromolecular systems through various strategies. As examples: the introduction of furfurylamine into the reaction of bisphenol-A diglycidyl ether (BADGE) was reported to form pendant furan functional oligomers;[14] multi-functional small molecule furan monomers for step-growth networks have been formed *via* direct esterification of 2-furoyl chloride and polyols;[15] post polymerisation modification of amine functional polyoxazolines using 3-(2-furyl)propanoic acid has been also been reported to form linear polymers with pendant furfuryl groups;[16] polyesters with furan end groups have been synthesised using telechelic isocyanate functional polymers and furfuryl alcohol;[17] and furfuryl glycidyl ether has been copolymerised through amine initiated BADGE reactions.[18]

Many monofunctional furans can be made directly from furfural, an inherently renewable aldehyde feedstock derived from lignocellulose biomass.[19,20] Furfuryl alcohol is readily converted to furfuryl methacrylate (FMA) *via* reaction with methacrylic acid, which may also be sourced from biomass-derived glucose,[21] making FMA an extremely attractive monomer for polymers targeting D–A reactions.

Conventional free radical polymerisation (FRP) currently represents approximately 45% of plastic and 40% of synthetic rubber manufacture globally.[22] FMA is well known to undergo

[a]Department of Chemistry, University of Liverpool, Liverpool, UK.
E-mail: srannard@liverpool.ac.uk
[b]Department of Chemistry, The University of Sheffield, Sheffield, UK
[c]Becker Industrial Coatings Ltd, Beckers Group, Liverpool, UK

side reactions during FRP leading to gel formation even at low to moderate conversion.[23] Due to the presence of the vinyl functionality within the furan ring, radical addition may occur leading to network formation.[24] Homopolymerisation is particularly hampered by side reactions and the formation of furyl radicals, predominantly at the C_5 ring position;[25] however, similar issues are also seen during copolymerisation. Several reports of styrene/FMA copolymerisations have observed crosslinking at relatively high concentrations of FMA. When methyl methacrylate (MMA) was polymerised under FRP conditions in the presence of increasing amounts of furfuryl acrylate a significant decrease in number-average molecular weight (M_n) and rate of polymerisation was observed, suggesting retardation due to chain transfer to the C_5 ring carbon.[25] To enable the use of furfuryl methacrylate in a range of applications, reversible-deactivation radical polymerisation (RDRP) techniques have been relied upon for some years. Initial reports compared AIBN-initiated FRP of FMA (insoluble polymer formed) against atom transfer radical polymerisation (ATRP) leading to soluble homopolymer (50% conversion), linear evolution of M_n with conversion, and a lack of reaction of the pendant furan ring under ATRP conditions. This same report also showed that statistical FMA/MMA copolymerisation (20 : 80 FMA/MMA molar ratio) under FRP conditions also led to a crosslinked product, whereas ATRP allowed soluble copolymer formation (58% conversion) with 23 mol% FMA and no apparent reaction of the furan ring.[26] Since this report, a wide range of FMA-containing polymer architectures have been generated using ATRP, and numerous groups have utilised RDRP to avoid the inherent side reactions of FMA in the presence of FRP conditions. Examples include: surface functionalisation of multi-walled carbon nanotubes using poly(furfuryl methacrylate), *p*(FMA), synthesised using reversible addition–fragmentation chain transfer (RAFT) polymerisation;[27] formation of transparent, conductive composite films using FMA/2-(dimethylamino)ethyl methacrylate statistical copolymers synthesised using ATRP; single chain "folded" nanoparticles utilising RAFT and ATRP to synthesise MMA/FMA/maleimide functionalized methacrylate terpolymers;[28] self-assembled drug loaded nanoparticles of maltoheptaose/FMA block copolymers synthesised using single electron transfer living radical polymerisation;[29] debondable adhesives utilising ATRP synthesised *p*(FMA); and RAFT-synthesised FMA/ethyl acrylate statistical copolymers within D–A networks containing "molecular springs".[30]

Recently, we reported the introduction of Transfer-dominated Branching Radical Telomerisation (TBRT) which utilises FRP chemistries under telomerisation conditions.[31] In summary, TBRT allows the formation of fully soluble high molecular weight branched polymers from the homopolymerisation or copolymerisation of multi-vinyl monomers, known as multi-vinyl taxogens (MVTs) under telomerisation conditions (Scheme 1).[32] Complete consumption of vinyl groups[33] without gelation appears to contradict Flory–Stockmayer theory;[34] however, TBRT is dominated by chain-transfer reactions between thiols (known as telogens) and high telogen con-

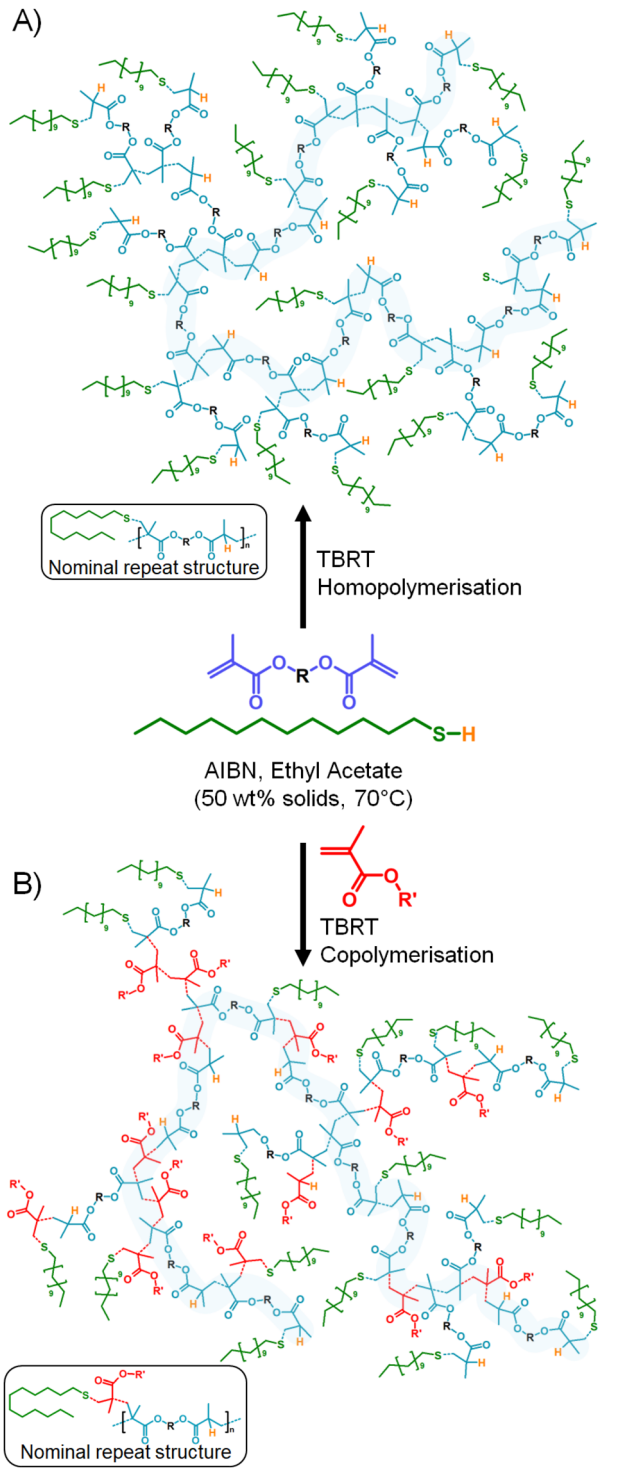

Scheme 1 Synthesis of branched polyesters *via* (A) TBRT homopolymerisation of multi-vinyl taxogens (MVT), and (B) TBRT copolymerisation using a mixed MVT/mono-VT feedstock. Dotted bonds signify bonds formed during limited propagation under telomerisation conditions and are provided to aid the reader. Blue highlights illustrate the extended polyester nature of the backbone. Nominal repeat structures are shown to simplify the complex branched architecture.

centration controls the kinetic chain length derived from vinyl propagation to very short chain lengths.[35] MVT structure,[36,37] telogen chemistry,[38] reaction temperature,[39] and concentration[40] have all been shown to influence the outcomes of TBRT reactions.

Importantly, TBRT of MVTs generates branched macromolecular backbones that resemble step-growth polymers as the carbon–carbon bond formation resulting from limited propagation merely links together the chemistry already present within the MVT feedstocks.

Put simply, a branched polyester is formed when a di(meth)acrylate MVT is used, and chemistries within the initial MVT may be deliberately placed in the backbone of the polymer by careful design or selection (Scheme 1A).[40–42] TBRT therefore offers the benefits of FRP, namely speed of reaction, highly diverse commercially available feedstocks, and ready scalability, with the added advantage of forming analogous step-growth (co)polymers with pendant functional groups. We have recently shown that pendant ATRP initiators may be readily incorporated into branched polyesters through TBRT copolymerisation (Scheme 1B); the highly common MVT ethylene glycol dimethacrylate (EGDMA) was copolymerised with 2-(α-bromoisobutyryloxy)ethyl methacrylate (a mono-VT inimer) under 1-dodecanethiol (DDT) telogen control[43] without any loss of pendant tertiary bromo functionality. Here we aimed to study FMA copolymerisation under TBRT conditions and establish the potential for sensitive unsaturated functional group compatibility within this new branched polymer chemistry.

Results and discussion

Synthesis of *p*([DDT-EGDMA]-*stat*-FMA) copolymers

As mentioned above, mixed MVT/mono-VT copolymerisations offer a facile route to introduce pendant functionality into branched polymers bearing backbones analogous to step-growth materials. FMA was, therefore, copolymerised with EGDMA in a 1 : 1 molar ratio in the presence of DDT using an $[EGDMA]_0/[DDT]_0$ molar ratio of 0.83. The copolymerisation was initiated using 2,2′-azobis(isobutyronitrile) (AIBN), at 1.5 mol% *vs.* vinyl functional groups and conducted at 70 °C in ethyl acetate at 50 wt% (Scheme 2).

TBRT using EGDMA and DDT has been reported several times,[31,33,35,36,39,40,42] allowing direct understanding of the impact of the addition of FMA. This is very important given the potential for reaction at the furan ring and modification of the TBRT pathway. In the absence of FMA, the TBRT of EGDMA/DDT under these conditions is known to undergo gelation at an $[EGDMA]_0/[DDT]_0$ feedstock ratio >0.85, whilst a molar ratio of 0.83 consumes all vinyl functional groups and generates soluble branched polymers with high weight-average molecular weights (M_w).

Here, the copolymerisation reaction ($[EGDMA]_0/[DDT]_0$ = 0.83/$[FMA]_0/[EGDMA]_0$ = 1.00) did indeed generate a soluble branched product with >99% consumption of the vinyl functionality as determined by ^{1}H nuclear magnetic resonance spectroscopy (NMR) after 24 hours (Fig. 1 & Fig. S1). We have previously drawn a distinction between conventional vinyl 'conversion' and the 'consumption' of vinyl groups within polymerisations such as TBRT. The disappearance of vinyl groups is conventionally correlated to the addition of free monomer to growing polymer chains and conversion of monomer to polymer. Within TBRT (co)polymerisations vinyl groups may be consumed through three mechanisms: (1) reaction of free monomer with growing polymer structures; (2) intermolecular branching *via* pendant vinyl groups; and (3) formation of DP_1 structural units that dominate TBRT polymers. As such, we believe that the term 'consumption' more appropriately reflects the relevant mechanistic processes occurring during TBRT.[38]

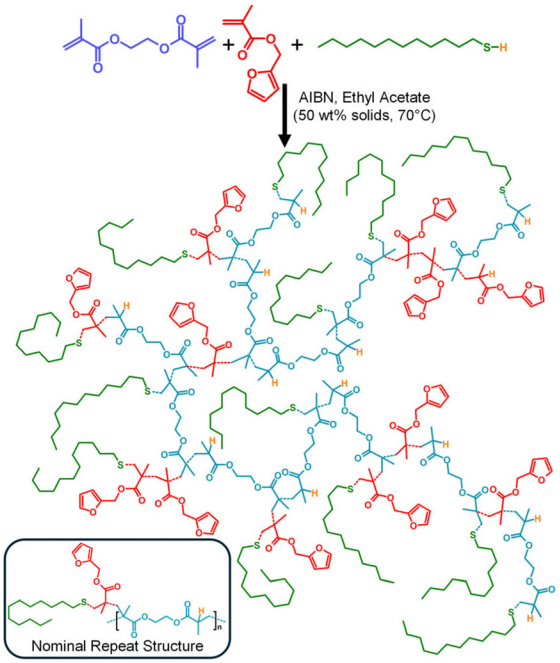

Scheme 2 Synthesis of *p*([DDT-EGDMA]-*stat*-FMA) using TBRT.

The fine balance of TBRT reactions conducted very close to the limiting gel point feedstock ratio (*i.e.* $[EGDMA]_0/[DDT]_0$ > 0.85) results in an obvious indication of additional intermolecular reaction by the formation of a gel network. At the $[EGDMA]_0/[FMA]_0$ molar ratio of 1 : 1 used here, the potential for FMA to contribute to branching would certainly have led to gelation if it were to act as a pseudo-MVT. The sample was purified to remove unreacted telogen and the soluble branched copolymer was analysed by triple-detection size exclusion chromatography (TD-SEC; Fig. 2A) and shown to have M_w = 679 550 g mol^{-1}; M_n = 5770 g mol^{-1}, dispersity ($Đ$) = 117.7, and a Mark–Houwink–Sakurada α = 0.33 (THF + 0.5 v/v% triethylamine mobile phase; flow rate = 1 mL min^{-1}). These values are within the range expected for TBRT of EGDMA/DDT (*cf.* $[EGDMA]_0/[DDT]_0$ = 0.825: M_w = 510 450 g mol^{-1}; M_n = 7100 g mol^{-1}; $Đ$ = 71.9; α = 0.32).[40]

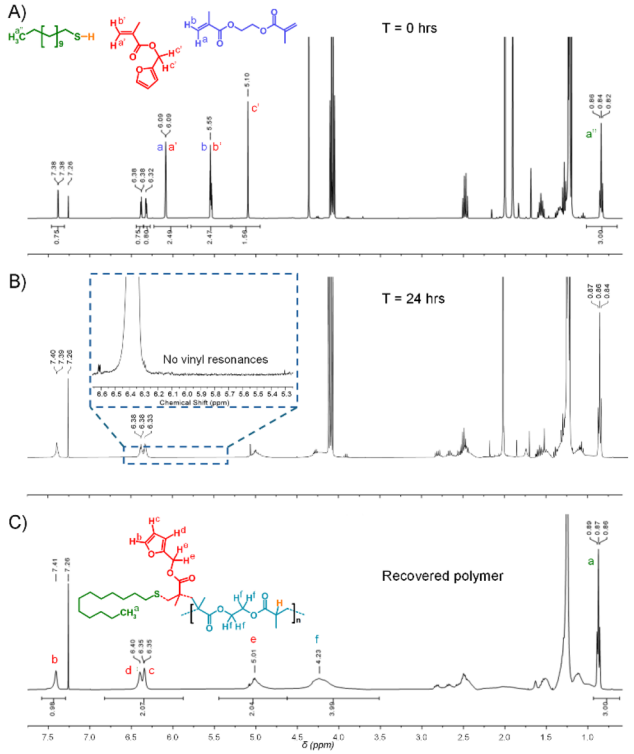

Fig. 1 ^{1}H NMR (400 MHz, $CDCl_3$) analysis of the synthesis of *p*([DDT-EGDMA]-*stat*-FMA). (A) Analysis of initial reaction mixture before addition of initiator (T = 0), utilised for the calculation of the feedstock ratio $[EGDMA]_0/[FMA]_0/[DDT]_0$; (B) Analysis of polymerisation mixture after 24 hours reaction time, showing full consumption of vinyl groups; (C) Purified polymer showing conservation of furfuryl functionality and final polymer composition *p*([$DDT_{1.00}$-$EGDMA_{1.00}$]-stat-$FMA_{1.04}$).

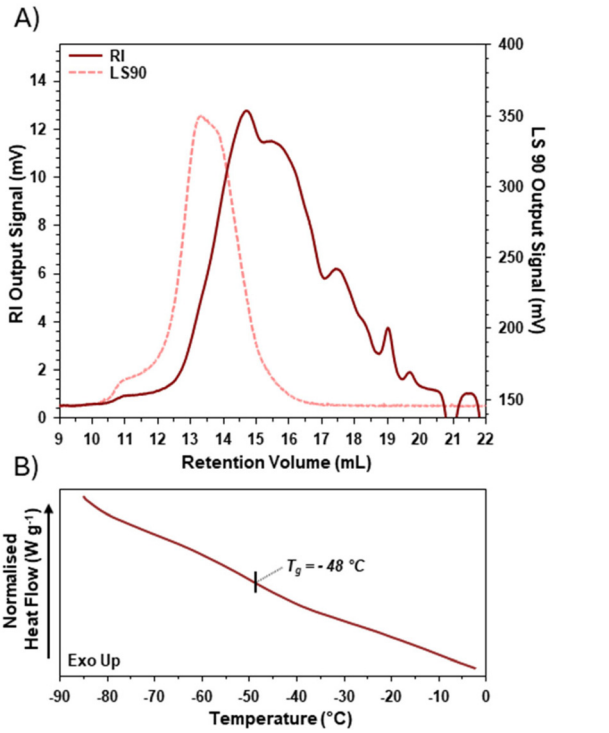

Fig. 2 Characterisation of *p*([DDT-EGDMA]-stat-FMA). (A) TD-SEC molecular weight analysis showing refractive index (RI) and right-angle light scattering (LS90) chromatograms (THF/0.5 v/v% TEA mobile phase; flow rate of 1 mL min^{-1}); (B) DSC thermogram of the second heat ramp of a heat-cool-heat cycle, performed at a rate of 10 °C min^{-1}.

Ideally, the composition of the purified copolymer was targeted as *p*([DDT-EGDMA]-*stat*-FMA) with a 1 : 1 : 1 molar ratio of each of the component feedstock elements. ^{1}H NMR characterisation showed *p*([$DDT_{1.00}$-$EGDMA_{1.00}$]-*stat*-$FMA_{1.04}$) for the recovered copolymer (Fig. S1), indicating preservation of the FMA diene functionality and a $[EGDMA]_{final}/[DDT]_{final}$ ratio = 1.00 which is indicative of ideal branching (no or highly limited cyclisation) within TBRT reactions (Fig. S2 & S3).[40] Evidence of reaction at the unsaturated furan functionality would be clear within the ^{1}H NMR spectrum as losses of H^b, H^c and H^d (Fig. 1C), and the appearance of new resonances attributed to the reaction products. There is, however, no clear evidence of hydrothiolation of the furan rings of FMA during TBRT, including within significant spectrum expansion and comparison against model reactions of 2-methyl furan and DDT under TBRT conditions (Fig. S4). This may be due to the dominant thiol–thiyl radical transfer reaction within TBRT, but addition work is required to confirm this mechanism.

Differential scanning calorimetry (DSC) studies of the copolymer showed a weak glass transition temperature (T_g) value of −48 °C (Fig. 2B), in close agreement with previously reported T_g values for *p*(DDT-EGDMA) homopolymers.[40] This suggests no or minimal restrictions to backbone mobility imparted by the pendant furan rings. In contrast, the inclusion of benzyl methacrylate (BzMA) into similar copolymers has shown a considerable increase in observed thermal transitions (*p*([$DDT_{1.0}$-$EGDMA_{1.0}$]-*stat*-$BzMA_{1.0}$): T_g = 12 °C).[33]

Diels–Alder model reactions to establish optimal study conditions

TBRT was able to incorporate FMA without any adverse side reactions, however, it was unclear whether the steric availability of the diene rings would be impacted by the complex branched architecture when attempting D–A coupling reactions.

To guide the D–A evaluation of *p*([DDT-EGDMA]-*stat*-FMA), small molecule model D–A solution reactions (DMSO-d_6) were conducted using maleimide (MI) and 2-methylfuran (MF) over a range of temperatures (23–90 °C). The MI/MF molar ratio was also varied from 1 : 1 to 1 : 3 with the association of MI determined by ^{1}H NMR spectroscopy after 24 hours equilibration at each temperature. Measurements were conducted as quickly as practically possible (approx. 5 minutes) after equilibration to mitigate changes in the product distributions that may occur during long periods of storage. The relative proportion of *endo*- and *exo*- diastereomeric adducts formed was also determined (Fig. 3 and Fig. S5, 6 and eqn (S1)–(S2)).

Under each molar ratio studied, association of MI was found to increase with increasing temperature up to 60 °C, for

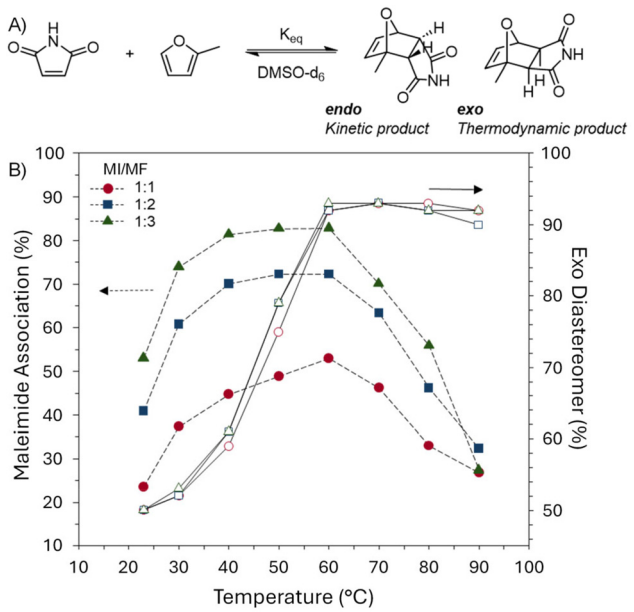

Fig. 3 Study of model D–A reaction using (A) maleimide (MI) and 2-methylfuran (MF). (B) Equilibrium position of D–A coupling at varying temperatures and reagent ratios, characterised by maleimide double bond consumption and *endo*/*exo* diastereomeric product ratio.

which the equimolar reaction achieved 53% MI association. Predictably, the association of MI was found to increase within increasing molar equivalents of MF, clearly acting to drive the D–A equilibrium towards adduct formation (60 °C: MI/MF = 1 : 2, MI association = 73%; MI/MF = 1 : 3, MI association = 83%). When using MI/MF ratios of 1 : 2 and 1 : 3, a clear plateau of MI association was observed between 40–60 °C, whereas measurements of the reaction conducted under equimolar conditions showed a steady increase of MI association to the maximum value at 60 °C. As can also be seen, temperatures >60 °C led to the increasing effect of the retro-Diels Alder reaction (rD–A), with equilibria tested at 90 °C showing remarkably consistent values of MI association (27–32%). For maleimide-furan D–A reactions, the endo- and exo-diastereomers are known to be kinetically and thermodynamically favoured, respectively.[44] The proportion of exo-diastereomer was estimated to be approximately 50% of the identified D–A adducts at ambient temperature, and became increasingly favoured up to 60 °C, where it contributed over 90% of the adduct distribution: this remained consistent at higher temperatures.

Overall, these studies suggest that an evaluation of the reactivity of furan functionality within *p*([DDT-EGDMA]-*stat*-FMA) would be optimally studied using a 1 : 1 molar ratio of diene and dienophile at 60 °C. Having an excess of diene within these studies may unduly lead to an overestimation of the D–A reactivity of the copolymer and crosslinking may be achieved predominantly through the most accessible diene groups; the D–A adducts formed would be expected to be heavily biased towards the exo-diastereomer under these conditions.

Diels–Alder evaluation of *p*([DDT-EGDMA]-*stat*-FMA) copolymers

The D–A reactivity of *p*([DDT-EGDMA]-*stat*-FMA) copolymers was studied in solution using the commercially available bifunctional dienophile 1,1′-(methylenedi-1,4-phenylene) bismaleimide (BMI). *p*([DDT-EGDMA]-*stat*-FMA) and BMI were dissolved in dimethyl formamide (DMF) at a 10 wt% concentration of the copolymer and 1 : 0.9 molar ratio of FMA residues/maleimide units (Fig. 4Ai). DMF was selected as a good, high boiling common solvent for both components, and the slight excess of diene was selected to overcome any inherent error in copolymer composition determination by ^{1}H NMR analysis. Under these conditions, we expected to consume all maleimide moieties present.

The copolymer/BMI solution was heated to 60 °C with stirring until macroscopic gelation occurred, demonstrated by the upturning of the vial and resultant lack of flow (Fig. 4Aii). This correlates well with conditions used in previous reports of the formation of D–A adduct precursors for epoxy-amine networks.[45] Subsequent heating of the gel to 120 °C resulted in a rapid liquification and recovery of a free-flowing solution (Fig. 4Aiii). The gelation/liquification process was able to be cycled as the D–A/rD–A equilibrium oscillated with heating and cooling (Fig. 4Aiv & v). The sol/gel remained transparent at all times demonstrating the high compatibility of *p*([DDT-EGDMA]-*stat*-FMA), BMI, and the crosslinked D–A adduct. An intensifying hue was seen with repeated heat/cool cycles, attributed to side reactions and oxidation of BMI.[46] As may be expected, the liquification of a preformed gel proceeded considerably faster than initial gelation and is probably related to two factors, namely (1) increasing viscosity during gelation leading to diffusion limited reaction of BMI and furan residues, and (2) the need for two reactions to undergo intermolecular crosslinking (BMI plus two furan rings), whereas only a single rD–A reaction is required to break the network at each crosslink site (Fig. 4Bi–iii).

Considerations of TBRT branched copolymer Diels–Alder reactions

Two specific features of the furan-functional polymer synthesised here are worth consideration. Firstly, the broad molecular weight distribution ensures that a fraction of the polymer is represented by very large, branched macromolecules, whilst the most common species is still relatively small (Fig. 4Bi). TBRT polymers can be represented by a nominal repeating structure (Schemes 1 and 2), and this is very simple to identify when considering an equimolar ratio of components within the copolymer (Scheme 1 & Fig. 4). The nominal repeat unit of the *p*([DDT-EGDMA]-*stat*-FMA) copolymer studied here has a molecular weight of 566.81 g mol^{-1} (equivalent to one DDT, one EGDMA, and one FMA), therefore the number-average structure within the distribution has approximately 10 furan groups per molecule, whilst the weight-average structures have nearly 1200 furan functional groups. Rapid molecular weight growth would be expected during D–A crosslinking, and gela-

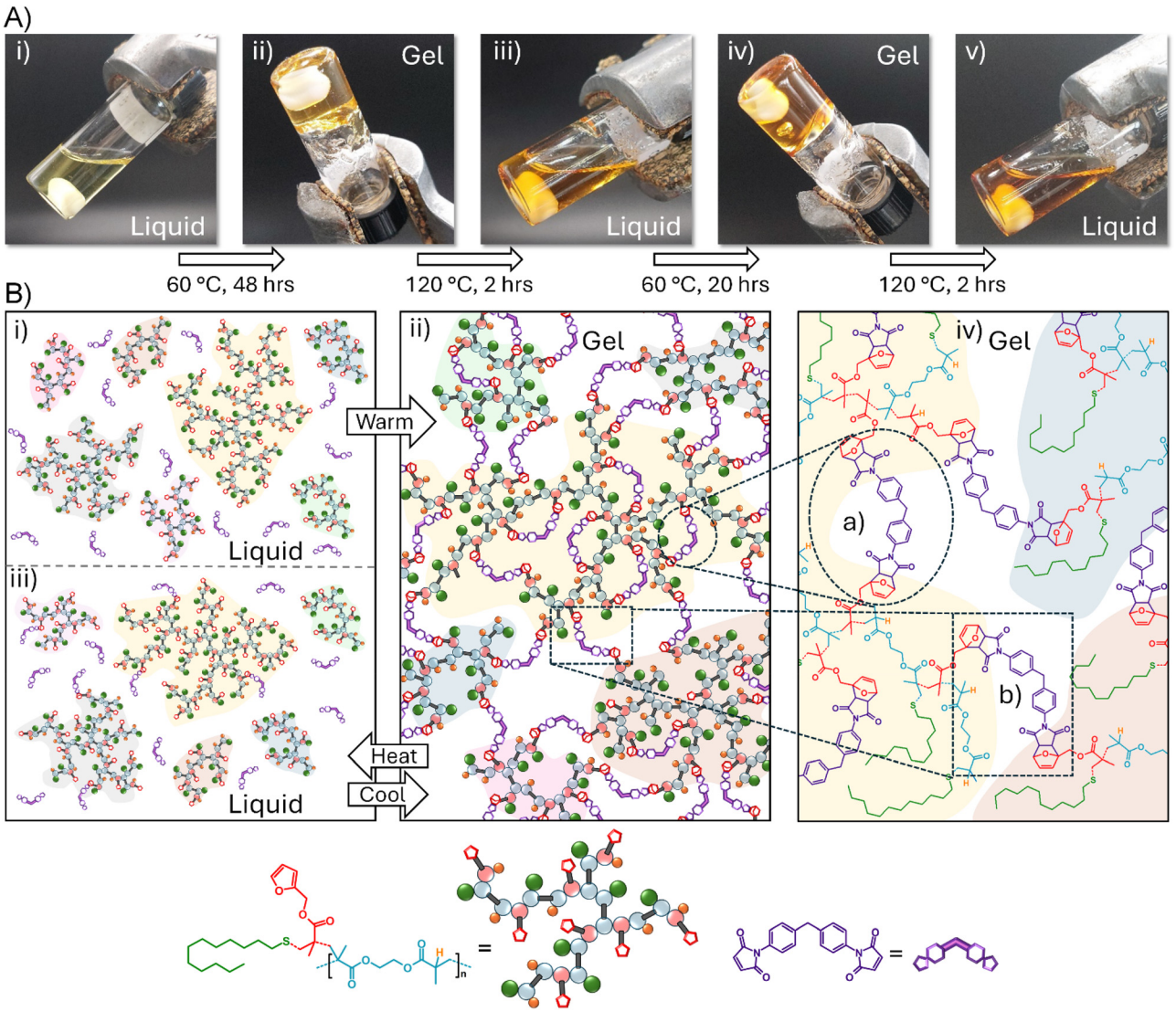

Fig. 4 Evaluation of reversible Diels–Alder (D–A) coupling/network formation. (A) Photographs showing reversible gelation of *p*([DDT-EGDMA]-stat-FMA) in solution: (Ai) initial dissolution of *p*([DDT-EGDMA]-stat-FMA) with BMI in DMF; (Aii) first gelation, after stirring at 60 °C for 48 h; (Aiii) first retro Diels–Alder (rD–A) liquification, after heating to 120 °C for 2 h; (Aiv) second gelation, after heating at 60 °C for 20 h, and Av) second rD–A, after returning to 120 °C for 2 h. (B) Schematic of the reversible D–A/rD–A network formation: (Bi) solution of a broad distribution of branched, diene-functional macromolecules and BMI dienophile; (Bii) network formation showing connectivity between branched polymers *via* intermolecular D–A adduct formation (square dotted box) and the creation of macrocycles *via* intramolecular D–A reaction (dotted oval); (Biii) rD–A products upon heating of network showing the presence of BMI and mono-adducts still attached to branched polymers; (Biv) Depiction of chemical structure of the network, including intramolecular D–A cyclic adduct formation (a) dotted oval and intermolecular crosslinking (b) square dotted box.

tion would be expected at low levels of reaction (Fig. 4Bii), given the dependence of the modified Carothers equation on the average functionality of the crosslinking reactants.[47] Conversely, the rD–A reaction would be expected to generate a relatively free flowing liquid given the M_n of the copolymer, and this is indeed seen. The nominal repeat unit molecular weight also represents the 'furan-equivalent molecular weight' (*cf.* epoxy equivalent molecular weight),[48] however, unlike many commercial resins, the functionality is not limited to the ends of small molecules or low molecular weight oligomers.[49] From a weight fraction perspective, approximately 50% of the mass of the polymer sample has a molecular weight >100 000 g mol^{-1}, equating to >175 furan rings/molecule; approximately 10 wt% represents molecules with a molecular weight >1 000 000 g mol^{-1} bearing >1760 furan groups (Fig. S7).

Secondly, intramolecular cyclisation would be expected during the formation of the D–A adducts, given the large density of furan groups and their relative proximity within the complex distribution of architectures (Fig. 4Bii & iv). Although cyclisation is somewhat inevitable, at this stage of our analysis it does not seem to impair gelation. Indeed, in the final network, there may be very little obvious structural difference between intramolecular D–A adduct formation (Fig. 4Biv-a)

and intermolecular crosslinking (Fig. 4Biv-b), with both acting as load-bearing structures. This may provide a benefit over conventionally cured networks as the formation of so called 'dangling loops',[50] or cycles that do not contribute to the mechanical properties of the network,[51] is somewhat limited. Intramolecular D–A adduct formation in the branched copolymer studied here will restrict motion and add to the rigidity of the branched macromolecule polyester backbone;[52] numerous cycles of this type would be expected to impact homogenously across the final network and increase the final T_g of the crosslinked polymer and will require further study.

Conclusions

Although furfuryl methacrylate has been utilised in many chain-growth copolymer reports of reversible crosslinking *via* Diels–Alder coupling, the need to avoid side reactions has predominantly relied upon controlled radical chemistries which may not be readily applicable at industrial scales, and limited large-scale demonstrations of these techniques have been reported.[53,54] We have shown here the first use of conventional free radical chemistries in the formation of branched furan-functional resins with step-growth backbones (polyester) without substantial side reactions. TBRT clearly offers new synthetic scope for functional step-growth D–A resin manufacture. The reversible gelation studies indicate that the furan groups are accessible, and the material formed may act as a foundation for further materials evaluation. Our studies will focus on systematic variation of structure, molecular weight, and functionality and their impact on the properties of solid covalent adaptable networks that may be formed.

Author contributions

OBP-L was responsible for conceptualisation, methodology, experimentation, investigation, data curation, formal analysis and visualisation, and preparation of the original draft. SL contributed to experimental work. SW, ATS contributed to validation and scrutiny of data. AD contributed to supervision, project administration, analytical services and validation. SPR was responsible for funding acquisition, conceptualisation of the research programme, methodology, validation, visualisation, supervision, project administration, manuscript review and editing.

Conflicts of interest

SPR and SW are co-inventors on patents that protect TBRT chemistry.

Data availability

The data supporting this article have been included within the manuscript or as part of the supplementary information (SI). Supplementary information including experimental procedures, nuclear magnetic resonance spectroscopy of reaction mixtures and purified polymers, FT-IR spectra, measurements of Diels-Alder equilibria, and SEC analysis is available. See DOI: https://doi.org/10.1039/d6py00258g.

Acknowledgements

The Engineering & Physical Sciences Research Council (EPSRC) are gratefully acknowledged for funding through grant EP/X010864/1. The authors would like to thank the Materials Innovation Factory (University of Liverpool) for analytical support.

References

1 O. Diels and K. Alder, *Justus Liebigs Ann. Chem.*, 1928, **460**, 98.
2 K. C. Nicolaou, S. A. Snyder, T. Montagnon and G. Vassilikogiannakis, *Angew. Chem., Int. Ed.*, 2002, **41**, 1668.
3 A. Rana, A. Mishra and S. K. Awasthi, *RSC Adv.*, 2025, **15**, 4496.
4 M. Gregoritza and F. P. Brandl, *Eur. J. Pharm. Biopharm.*, 2015, **97**, 438.
5 J. A. Funel and S. Abele, *Angew. Chem., Int. Ed. Engl.*, 2013, **52**, 3822.
6 J. Lopez-Sanchez, M. Alajarin, A. Pastor and J. Berna, *J. Org. Chem.*, 2021, **86**, 15045.
7 S. Schäfer and G. Kickelbick, *ACS Appl. Nano Mater.*, 2018, **1**, 2640.
8 M. A. Tasdelen, *Polym. Chem.*, 2011, **2**, 2133.
9 Y.-L. Liu and T.-W. Chuo, *Polym. Chem.*, 2013, **4**, 2194.
10 C. R. Ratwani, A. R. Kamali and A. M. Abdelkader, *Prog. Mater. Sci.*, 2023, **131**, 101001.
11 S. M. Morozova, *Gels*, 2023, **9**, 102.
12 A. Degirmenci, R. Sanyal and A. Sanyal, *RSC Appl. Polym.*, 2024, **2**, 976.
13 E. J. Corey, *Angew. Chem., Int. Ed.*, 2002, **41**, 1650.
14 G. Zhang, Q. Zhao, L. Yang, W. Zou, X. Xi and T. Xie, *ACS Macro Lett.*, 2016, **5**, 805.
15 T. Höfer, A. Rössler and O. I. Strube, *ACS Polym. Au*, 2026, **6**, 315.
16 Y. Chujo, K. Sada and T. Saegusa, *Macromolecules*, 1990, **23**, 2636.
17 M. Watanabe and N. Yoshie, *Polymer*, 2006, **47**, 4946.
18 A. M. Peterson, R. E. Jensen and G. R. Palmese, *ACS Appl. Mater. Interfaces*, 2010, **2**, 1141.
19 R. Mariscal, P. Maireles-Torres, M. Ojeda, I. Sádabaa and M. López Granados, *Energy Environ. Sci.*, 2016, **9**, 1144.
20 A. Gandini, D. Coelho, M. Gomes, B. Reis and A. Silvestre, *J. Mater. Chem.*, 2009, **19**, 8656.
21 Y. Wu, M. Shetty, K. Zhang and P. J. Dauenhauer, *ACS Eng. Au*, 2022, **2**, 92.
22 S. Liu, *Chem. Mater.*, 2024, **36**, 1779.
23 A. Gandini, *Adv. Polym. Sci.*, 1977, **25**, 78.

24 J. Lange, J. Rieumont, N. Davidenko and R. Sastre, *Polymer*, 1998, **39**, 2537.
25 N. Davidenko, D. Zaldivar, C. Peniche, R. Sastre and J. San Román, *J. Polym. Sci., Part A: Polym. Chem.*, 1996, **34**, 2759.
26 A. A. Kavitha, A. Choudhury and N. K. Singha, *Macromol. Symp.*, 2006, **240**, 232.
27 N. B. Pramanik and N. K. Singha, *RSC Adv.*, 2015, **5**, 94321.
28 A. M. Hanlon, I. Martin, E. R. Bright, J. Chouinard, K. J. Rodriguez, G. E. Patenotte and E. B. Berda, *Polym. Chem.*, 2017, **8**, 5120.
29 T. Lee, B. Kim, S. Kim, J. H. Han, H. B. Jeon, Y. S. Lee and H.-J. Paik, *Nanoscale*, 2015, **7**, 6745.
30 I. O. Raji, M. Eisenhart, R. Lama, G. P. Devkota, C. S. Hartley and D. Konkolewicz, *Macromolecules*, 2025, **58**, 12346.
31 S. R. Cassin, P. Chambon and S. P. Rannard, *Polym. Chem.*, 2020, **11**, 7637.
32 B. Boutevin, *J. Polym. Sci., Part A: Polym. Chem.*, 2000, **38**, 3235.
33 S. R. Cassin, S. Flynn, P. Chambon and S. P. Rannard, *Polym. Chem.*, 2022, **13**, 2295.
34 W. H. Stockmayer, *J. Chem. Phys.*, 1944, **12**, 125.
35 S. Cassin, S. Flynn, P. Chambon and S. P. Rannard, *RSC Adv.*, 2021, **11**, 24374.
36 O. B. Penrhyn-Lowe, S. Flynn, S. R. Cassin, S. Mckeating, S. Lomas, S. Wright, P. Chambon and S. P. Rannard, *Polym. Chem.*, 2021, **12**, 6472.
37 C. Smith, O. B. Penrhyn-Lowe, S. Mckeating, S. Wright, A. B. Dwyer and S. P. Rannard, *Polym. Chem.*, 2025, **16**, 1486.
38 S. Flynn, B. Linthwaite, O. B. Penrhyn-Lowe, S. Mckeating, S. Wright, S. R. Cassin, P. Chambon and S. P. Rannard, *Polym. Chem.*, 2023, **14**, 5102.
39 S. Flynn, O. B. Penrhyn-Lowe, S. Mckeating, S. Wright, S. Lomas, S. R. Cassin, P. Chambon and S. P. Rannard, *RSC Adv.*, 2022, **12**, 31424.
40 S. R. Cassin, S. Wright, S. Mckeating, O. B. Penrhyn-Lowe, S. Flynn, S. Lomas, P. Chambon and S. P. Rannard, *Polym. Chem.*, 2023, **14**, 1905.
41 S. Mckeating, O. B. Penrhyn-Lowe, S. Flynn, S. R. Cassin, S. Lomas, C. Fidge, P. Price, S. Wright, P. Chambon and S. P. Rannard, *Commun. Chem.*, 2024, **7**, 197.
42 O. B. Penrhyn-Lowe, S. R. Cassin, P. Chambon and S. Rannard, *Nanoscale Adv.*, 2022, **4**, 4051.
43 A. B. Dwyer, W. M. Sandy, F. Y. Hern, O. B. Penrhyn-Lowe, S. McKeating, S. Flynn, S. Wright, S. Pate, P. Chambon and S. P. Rannard, *Chem. Commun.*, 2024, **60**, 10116.
44 V. Froidevaux, M. Borne, E. Laborbe, R. Auvergne, A. Gandini and B. Boutevin, *RSC Adv.*, 2015, **5**, 37742.
45 A. Cuvellier, R. Verhelle, J. Brancart, B. Vanderborght, G. Van Assche and H. Rahier, *Polym. Chem.*, 2019, **10**, 473.
46 W. Shaoquan, D. Shangli, G. Yu and T. Ozbakkaloglu, *Compos. Part A Appl. Sci. Manuf.*, 2019, **119**, 235.
47 E. Meaurio, *J. Polym. Sci.*, 2025, **63**, 2543.
48 S.-A. Garea, A.-C. Corbu, C. Deleanu and H. Iovu, *Polym. Test.*, 2006, **25**, 107.
49 M. Fache, A. Viola, R. Auvergne, B. Boutevin and S. Caillol, *Eur. Polym. J.*, 2015, **68**, 526.
50 C. W. H. Rajawasam, O. J. Dodo, M. A. Sachini, N. Weerasinghe, I. O. Raji, S. V. Wanasinghe, D. Konkolewicz and N. D. Watuthanthrige, *Polym. Chem.*, 2024, **1**, 219.
51 F. Chen and W. D. Cook, *Eur. Polym. J.*, 2008, **44**, 1796.
52 S. Panyukov, *Macromolecules*, 2019, **52**, 4145.
53 W. Jakubowski, ACS Symposium Series, in *Controlled Radical Polymerization: Materials*, ed. K. Matyjaszewski, American Chemical Society, Washington, DC, 2012, vol. 1100, Chapter 13, p. 203.
54 G. Moad, *RAFT Polymerization*, eds G. Moad and E. Rizzardo, Wiley-VCH, Weinheim, 2021, 2, 1077.

